

# Dissecting the Core of the Tarantula Nebula with MUSE

Paul A. Crowther<sup>1</sup>  
 Norberto Castro<sup>2</sup>  
 Christopher J. Evans<sup>3</sup>  
 Jorick S. Vink<sup>4</sup>  
 Jorge Melnick<sup>5</sup>  
 Fernando Selman<sup>5</sup>

<sup>1</sup> Department of Physics & Astronomy,  
 University of Sheffield, United Kingdom

<sup>2</sup> Department of Astronomy, University of  
 Michigan, Ann Arbor, USA

<sup>3</sup> UK Astronomy Technology Centre,  
 Royal Observatory, Edinburgh, United  
 Kingdom

<sup>4</sup> Armagh Observatory, United Kingdom

<sup>5</sup> ESO

We provide an overview of Science Verification MUSE observations of NGC 2070, the central region of the Tarantula Nebula in the Large Magellanic Cloud. Integral-field spectroscopy of the central  $2 \times 2$  arcminute region provides the first complete spectroscopic census of its massive star content, nebular conditions and kinematics. The star formation surface density of NGC 2070 is reminiscent of the intense star-forming knots of high-redshift galaxies, with nebular conditions similar to low-redshift Green Pea galaxies, some of which are Lyman continuum leakers. Uniquely, MUSE permits the star formation history of NGC 2070 to be studied with both spatially resolved and integrated-light spectroscopy.

## Tarantula Nebula

The Tarantula Nebula (30 Doradus) in the Large Magellanic Cloud (LMC) is intrinsically the brightest star-forming region in the Local Group and has been the subject of numerous studies across the electromagnetic spectrum. Its low (half-solar) metallicity and high star formation intensity are more typical of knots in high-redshift star-forming galaxies than local systems thanks to its very rich stellar content (Doran et al., 2013). Indeed, 30 Doradus has nebular conditions that are reminiscent of the galaxies known as Green Peas. These are local extreme emission-line galaxies that are analogues of high-redshift, intensely star-forming galaxies, some of which have been con-

firmed as Lyman continuum leakers (for example, Micheva et al., 2017).

The Tarantula Nebula is host to hundreds of massive stars that power the strong H $\alpha$  nebular emission, comprising main sequence OB stars, evolved blue supergiants, red supergiants, luminous blue variables and Wolf-Rayet (WR) stars. The proximity of the LMC (50 kpc) permits individual massive stars to be observed under natural seeing conditions (Evans et al., 2011). The exception is R136, the dense star cluster at the LMC's core that necessitates the use of adaptive optics or the Hubble Space Telescope (HST; see Khorrami et al., 2017, Crowther et al., 2016). R136 has received particular attention since it hosts very massive stars ( $\geq 100 M_{\odot}$ ; Crowther et al., 2016) that are the potential progenitors of pair-instability supernovae and/or merging black holes whose gravitational wave signatures have recently been discovered with LIGO.

Star formation in the Tarantula Nebula began at least 15–30 Myr ago, as witnessed by the cluster Hodge 301, whose stellar content is dominated by red supergiants. There was an upturn in its rate of star formation within the last 5–10 Myr, which peaked a couple of Myr ago in NGC 2070, the central ionised region that hosts R136. Star formation is still ongoing, as witnessed by the presence of massive young stellar objects and clumps of molecular gas observed with ALMA (Indebetouw et al., 2013). The interplay between massive stars and the interstellar medium also permits the investigation of stellar feedback at high spatial and spectral resolutions (for example, Pellegrini, Baldwin & Ferland, 2011).

## MUSE observations of NGC 2070

NGC 2070, the central region of the Tarantula Nebula, was observed with the Multi Unit Spectroscopic Explorer (MUSE) as part of its original Science Verification programme at the Very Large Telescope (VLT) in August 2014. MUSE is a wide-field, integral-field spectrograph, providing intermediate-resolution ( $R \sim 3000$  at H $\alpha$ ) spectroscopy from 4600–9350 Å over one square arcminute with a pixel scale of 0.2 arcseconds. Four overlapping MUSE pointings provided a  $2 \times 2$  arcmin-

ute mosaic which encompasses both the R136 star cluster and R140 (an aggregate of WR stars to the north). See Figure 1 for a colour-composite of the central  $200 \times 160$  pc of the Tarantula Nebula obtained with the Advanced Camera for Surveys (ACS) and the Wide Field Camera 3 (WFC3) aboard the HST. The resulting image resolution spanned 0.7 to 1.1 arcseconds, corresponding to a spatial resolution of  $0.22 \pm 0.04$  pc, providing a satisfactory extraction of sources aside from R136. Four exposures of 600 s each for each pointing provided a yellow continuum signal-to-noise (S/N)  $\geq 50$  for 600 sources. A total of 2255 sources were extracted using SExtractor, while shorter 10- and 60-second exposures avoided saturation of strong nebular lines. Absolute flux calibration was achieved using V-band photometry from Selman et al. (1999). An overview of the dataset, together with stellar and nebular kinematics, is provided by Castro et al. (submitted to A&A).

## Spatially resolved nebular properties

We present colour-composite images extracted from the MUSE datacubes in Figure 2, highlighting the stellar content and ionised gas, respectively. Figure 2a samples 6640, 5710 and 4690 Å, such that most stars appear white except for cool supergiants (orange; for example, Melnick 9 in the upper left) and WR stars, which appear blue owing to strong HeII 4686 Å emission. Examples of the WR stars include R134 to the right of the central R136 star cluster and the R140 complex at the top, which hosts WN and WC stars, subsets of WR stars that have dominant lines of ionised nitrogen and ionised carbon respectively. In contrast, Figure 2b highlights the distribution of low-ionisation gas ([SII] 6717 Å, red), high-ionisation gas ([OIII] 5007 Å, blue) and hydrogen (H $\alpha$ , green). Green point sources generally arise from broad H $\alpha$  emission from WR stars and related objects.

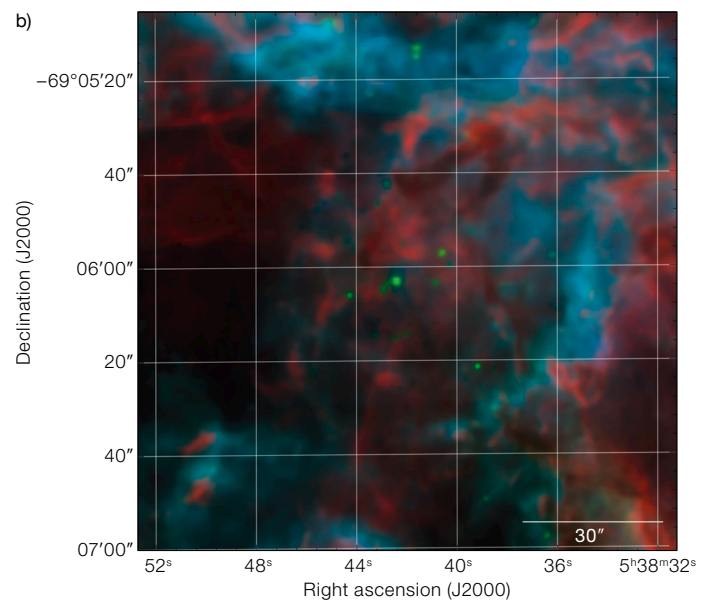
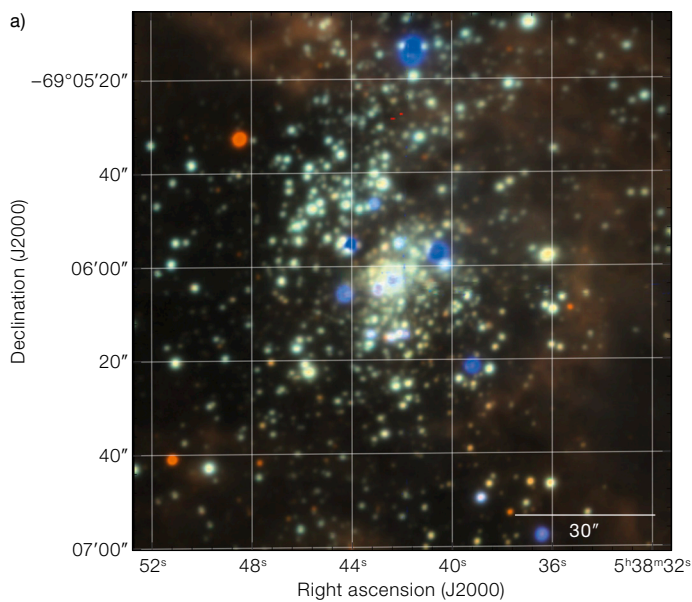
Owing to the presence of ionised gas throughout NGC 2070, our MUSE datasets enable the determination of nebular properties. Adopting a standard Milky Way extinction law, there is a wide variation in extinction throughout the region with



Figure 1. MUSE  $2 \times 2$  arcminute mosaic (white square) superimposed on a colour-composite image of the Tarantula Nebula (corresponding to  $\sim 200 \times 160$  parsecs), obtained with the ACS and WFC3 instruments aboard HST.<sup>1</sup>

Figure 2. (a) VLT/MUSE colour-composite image of NGC 2070 ( $2 \times 2$  arcminutes) sampling 6640 Å (red), 5710 Å (green), and 4690 Å (blue). Blue sources are WR stars with prominent HeII 4686 Å emission,

while orange sources are predominantly red supergiants. (b) VLT/MUSE colour-composite image of NGC 2070 ( $2 \times 2$  arcminutes) sampling [SII] 6717 Å (red), H $\alpha$  (green), and [OIII] 5007 Å (blue).



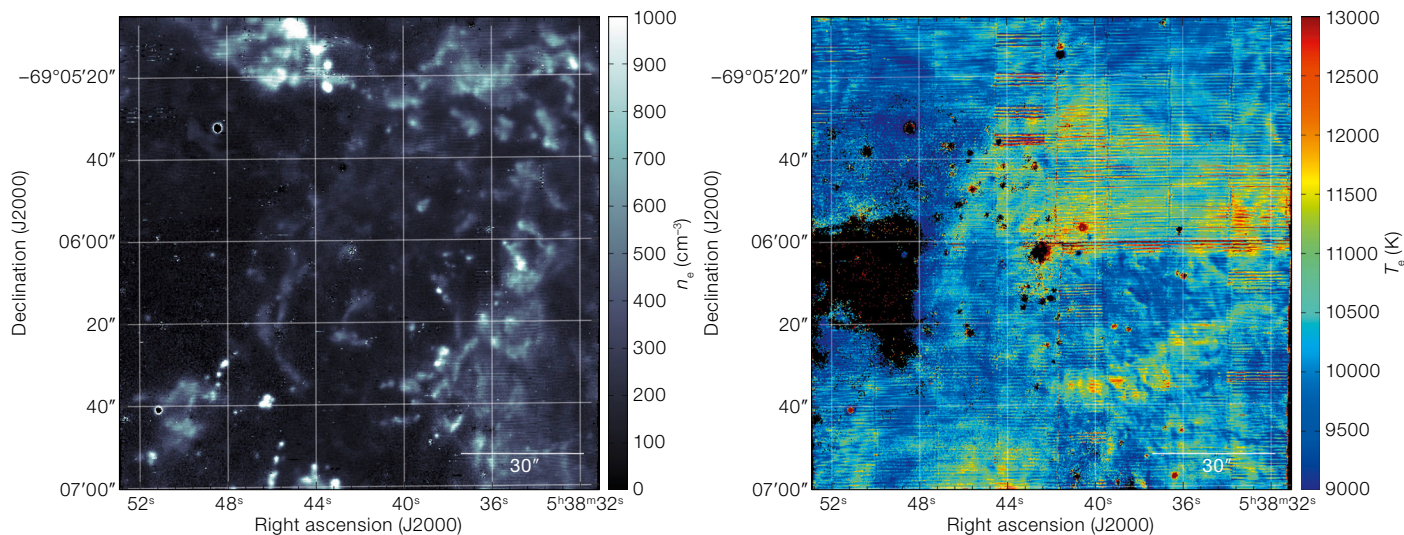
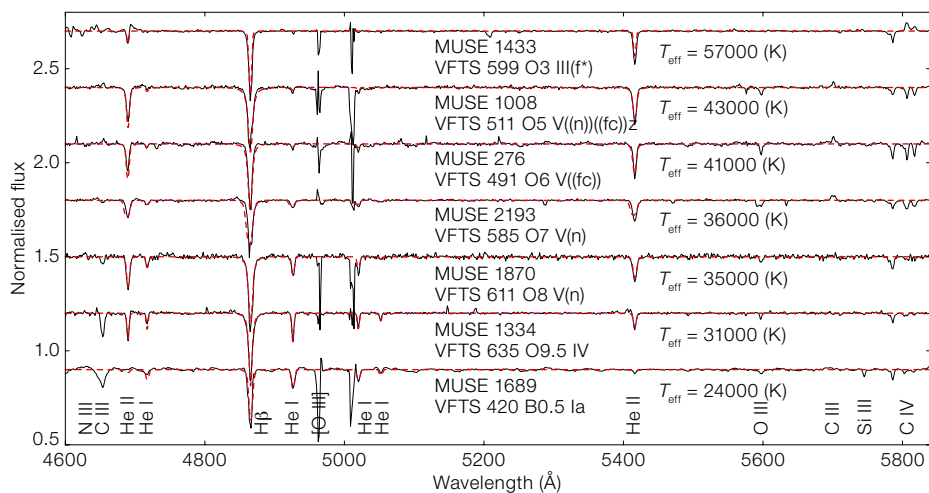


Figure 3. (Above) Distribution of gas density (left) and temperature (right) within the MUSE field of view, based on [S II] 6717/6731 Å and [S III] 6312/9069 Å diagnostics.

coefficients spanning  $0.15 \leq c(\text{H}\beta) \leq 1.2$ . On average, we found  $c(\text{H}\beta) = 0.55$  mag, which is in excellent agreement with long-slit results from Pellegrini, Baldwin & Ferland (2011). Nebular lines also permit the determination of electron densities and temperatures from [S II] and [S III] diagnostics as illustrated in Figure 3. The dust properties towards the Tarantula Nebula are known to be non-standard, with an average  $c(\text{H}\beta) = 0.6$  obtained from the law presented by Maíz-Apellániz et al. (2014) and  $R = 4.4$ , although this has little bearing on the nebular conditions determined here owing to the use of red spectral diagnostics.

### Massive stars in NGC 2070

MUSE permits the first complete spectroscopic census of massive stars within NGC 2070. Previous surveys have been restricted to multi-object spectroscopy using slitlets or fibres (Bosch et al., 1999; Evans et al., 2011). Spectral lines in the blue are usually employed in the classification of OB stars, so the 4600 Å blue limit to MUSE has required the development of green and yellow diagnostics. Representative OB spectra from MUSE are presented in Figure 4 with classifications from blue spectroscopy using the Fibre Large Array Multi Element Spectro-



graph (FLAMES) on the VLT (Walborn et al., 2014). A spectroscopic analysis of 270 sources with He II 5412 Å absorption is now underway using the non-local thermodynamic equilibrium atmospheric code FASTWIND (Puls et al., 2005), yielding temperatures and luminosities from He I 4921 Å and He II 5412 Å. Preliminary fits to the illustrative spectra are also shown in Figure 4.

Ultimately we will determine the properties of all of the massive stars in NGC 2070 in order to fully characterise its recent star-formation history, substituting results from long-slit HST spectroscopy using the Space Telescope Imaging Spectrograph (STIS) for the central parsec of R136 (Crowther et al., 2016). Quantitative analysis of the MUSE data should also provide useful insights to incorporate into

Figure 4. Blue to yellow spectroscopy of representative OB stars in NGC 2070 observed with VLT/MUSE (black solid lines), including spectral types from the VLT-FLAMES Tarantula survey, and temperatures from FASTWIND model fits (dashed red lines) to He I 4921 Å and He II 5412 Å.

stellar evolution theory. For instance, Castro et al. (2014) suggested empirical boundaries for the zero- and terminal-age main sequences from their analysis of a large sample of OB stars. The MUSE data will enable a homogeneous analysis of a larger stellar sample, spanning a broad range of evolutionary stages (for example, main sequence, blue and red supergiants, and WR stars).

Of course, it is well known that massive stars prefer company, so it is likely that many of the MUSE point sources are multiple. Fortunately, the majority of

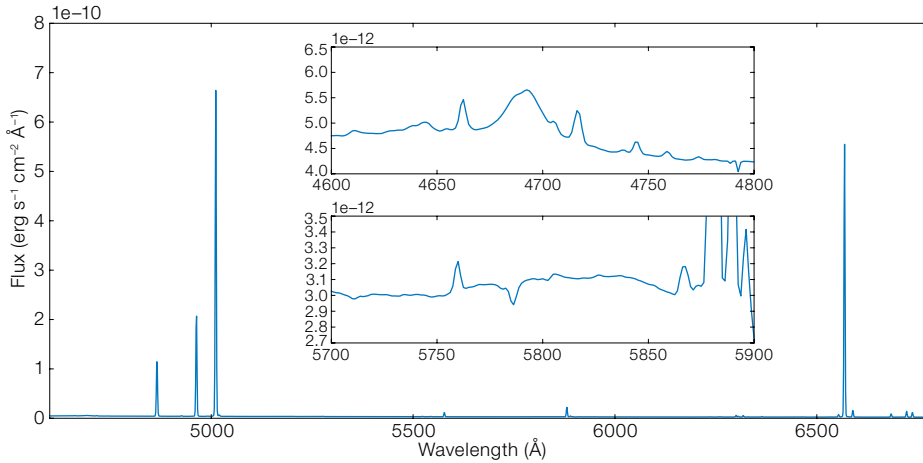


Figure 5. Integrated MUSE spectrum of NGC 2070, revealing a striking emission line spectrum, with characteristics reminiscent of Green Pea galaxies, plus WR bumps in the blue (upper inset, He II 4686 Å arising from WN stars) and yellow (lower inset, C IV 5801–12 Å due to WC stars).

massive stars in NGC 2070 have previously been monitored spectroscopically with VLT/FLAMES, revealing many short-period systems. In addition, 30 Doradus has been the target of the Chandra X-ray Visionary Programme (T-ReX) using the Advanced CCD Imaging Spectrometer (ACIS-I). This programme monitored X-ray emission from the Tarantula Nebula over 630 days, permitting longer-period systems to be identified. For example, Melnick 34, the blue emission-line star to the left of R136 in Figure 2a, has been revealed as an eccentric colliding-wind binary by its T-ReX variability (Pollock et al., 2017).

### Integrated spectrum of NGC 2070

In addition to spectra of the spatially-resolved stars and gas in NGC 2070, it is possible to sum the MUSE observations to arrive at the integrated spectrum of the region. NGC 2070 would subtend 0.6 arcseconds if it were located at a distance of 10 Mpc, so MUSE offers the unique opportunity to study both the spatially-resolved properties of an intensively star-forming region and its aggregate characteristics. The integrated spectrum of NGC 2070 is presented in Figure 5. In addition to strong nebular lines, the high throughput of MUSE and the proximity of NGC 2070 allow a plethora of weaker features to be revealed in the integrated spectrum, including the non-standard density diagnostic C III 5517/5537 Å. Figure 5 also highlights broad blue (He II 4686 Å) and yellow (C IV 5801–12 Å) WR features in the integrated spectrum, with no evidence for a nebular contribution

to the former. These are often observed in the integrated light of extragalactic star-forming regions.

Figure 6a compares the strong-line nebular characteristics of NGC 2070 with Sloan Digital Sky Survey (SDSS) star-forming galaxies and indicates similar high-excitation properties to those of Green Pea galaxies (Micheva et al., 2017). Analysis of the integrated spectrum reveals  $c(\text{H}\beta) = 0.57$  for a standard extinction law, such that the dereddened  $\text{H}\alpha$  luminosity is  $1.5 \times 10^{39}$  erg  $\text{s}^{-1}$ , corresponding to one-eighth of the entire Tarantula Nebula (Doran et al., 2013). The current star formation rate (SFR) for NGC 2070 is  $0.008 M_{\odot} \text{ yr}^{-1}$ . This has been obtained by adopting a standard Kennicutt (1998) relation between  $\text{H}\alpha$  luminosity and SFR, modified for a Kroupa (2002) initial mass function by dividing by a factor of 1.5, and inferring a high star formation surface density of  $\Sigma_{\text{SFR}} \sim 10 M_{\odot} \text{ yr}^{-1} \text{ kpc}^{-2}$ . Conditions are similar to clumps of intensively star-forming galaxies at high redshifts, as demonstrated in Figure 6b (adapted from Johnson et al., 2017).

### Properties inferred from the integrated light of NGC 2070

The inferred age of the region from the equivalent width of  $\text{H}\alpha$  is  $\sim 4$  Myr, implying a mass of  $10^5 M_{\odot}$  for an instantaneous burst of star formation. This is double the mass estimated for the central R136 cluster. In reality, there is an age spread of 0–10 Myr for massive stars within the entire Tarantula Nebula (Schneider et al.,

2017), although the peak of star formation was inferred to be  $\sim 4.5$  Myr ago, excluding R136 (which has an age of  $\sim 1.5$  Myr; Crowther et al., 2016). The  $\text{H}\alpha$ -derived ionising output is  $10^{51}$  photons  $\text{s}^{-1}$  for NGC 2070, equivalent to  $\sim 100$  O7 V stars. This corresponds to  $\sim 300$  O stars for the nebular derived age (Schaerer & Vacca, 1998), in good agreement with the number of MUSE sources that display He II 5412 Å absorption, albeit neglecting the (significant) contribution of the WR stars to the cumulative ionising output.

We derive  $\log(\text{O}/\text{H}) + 12 = 8.25$  for NGC 2070, adopting  $\text{N}^+$  and  $\text{S}^{++}$  temperatures for singly- and doubly-ionised oxygen, respectively. However, the blue MUSE cutoff excludes the use of the stronger [O III] 4363 Å line. Direct determinations for the entire 30 Doradus region indicate a somewhat higher oxygen content (for example,  $\log(\text{O}/\text{H}) + 12 = 8.33$ ; Tsamis et al., 2003). Since WR line luminosities are metallicity dependent (Crowther & Hadfield, 2006) one would infer 20 mid-WN and five early WC stars in NGC 2070, or  $\text{N}(\text{WR})/\text{N}(\text{O}) \geq 0.08$ , by adopting LMC templates. This is in reasonable agreement with the resolved WR content of the MUSE field, namely 10 WN stars, 6 Of/WN stars and 2 WC stars. The rich star cluster R136 hosts four of the most massive WN5h stars in the region, but only contributes one third of the cumulative He II 4686 Å emission. In contrast, the less prominent R140 complex, which hosts two WN6 stars and one WC star, contributes another third of the He II 4686 Å emission and dominates the integrated C IV 5808 Å and C III 4650 Å flux. This arises from the relatively weak wind strengths of main sequence WN5h stars, as opposed to the significantly stronger emission from classical WN stars.

Strong-line calibrations are widely employed to infer the metallicity of extragalactic H II regions because of the faintness of auroral lines. Application of the commonly used calibrations from Pettini & Pagel (2004), using the N2 and

O3N2 indices, would imply a Small Magellanic Cloud (SMC)-like oxygen content of  $\log(O/H) + 12 = 8.0$ , significantly lower than our direct determination. If one had to rely on strong-line diagnostics for NGC 2070, the use of SMC-metallicity WR templates from Crowther & Hadfield (2006) would suggest an unrealistically high number of mid-WN stars, and, in turn,  $N(WR)/N(O) \geq 0.3$ . This would represent a severe challenge to current single/binary population synthesis models for a starburst region with  $0.2 Z_{\odot}$ , in stark contrast with the  $N(WR)/N(O) \sim 0.07$  and  $0.4 Z_{\odot}$  that has been obtained from our spatially resolved spectroscopy of the region.

#### References

- Baldwin, J. A., Phillips, M. M. & Terlevich, R. 1981, *PASP*, 93, 5  
 Bosch, G. et al. 1999, *A&AS*, 137, 21  
 Castro, N. et al. 2014, *A&A*, 570, 13  
 Crowther, P. A. et al. 2016, *MNRAS*, 458, 624  
 Doran, E. et al. 2013, *A&A*, 558, A134  
 Evans, C. J. et al. 2011, *A&A*, 530, A108  
 Kennicutt, R. C. 1998, *ARA&A*, 36, 189  
 Khorrami, Z. et al. 2017, *A&A*, 602, A56  
 Kroupa, P. 2002, *Science*, 295, 82  
 Indebetouw, R. et al. 2013, *ApJ*, 774, 73  
 Johnson, T. L. et al. 2017, *ApJ*, 843, L21  
 Maíz-Apellániz, J. et al. 2014, *A&A*, 564, A63  
 Micheva, G. et al. 2017, *ApJ*, 845, 165  
 Pellegrini, E. W., Baldwin, J. A. & Ferland, G. J. 2011, *ApJ*, 738, 34  
 Pettini, M. & Pagel, B. E. J. 2004, *MNRAS*, 348, L59  
 Puls, J. et al. 2005, *A&A*, 435, 669  
 Pollock, A. M. T. et al. 2017, *MNRAS*, in press  
 Schaerer, D. & Vacca, W. D. 1998, *ApJ*, 497, 618  
 Selman, F. et al. 1999, *A&A*, 341, 98  
 Schneider, F. et al. 2017, *Science*, in press  
 Tsamis, Y. et al. 2003, *MNRAS*, 338, 687  
 Walborn, N. et al. 2014, *A&A*, 564, A40

#### Links

- <sup>1</sup> Hubble News Release:  
<https://www.spacetelescope.org/news/heic1206>

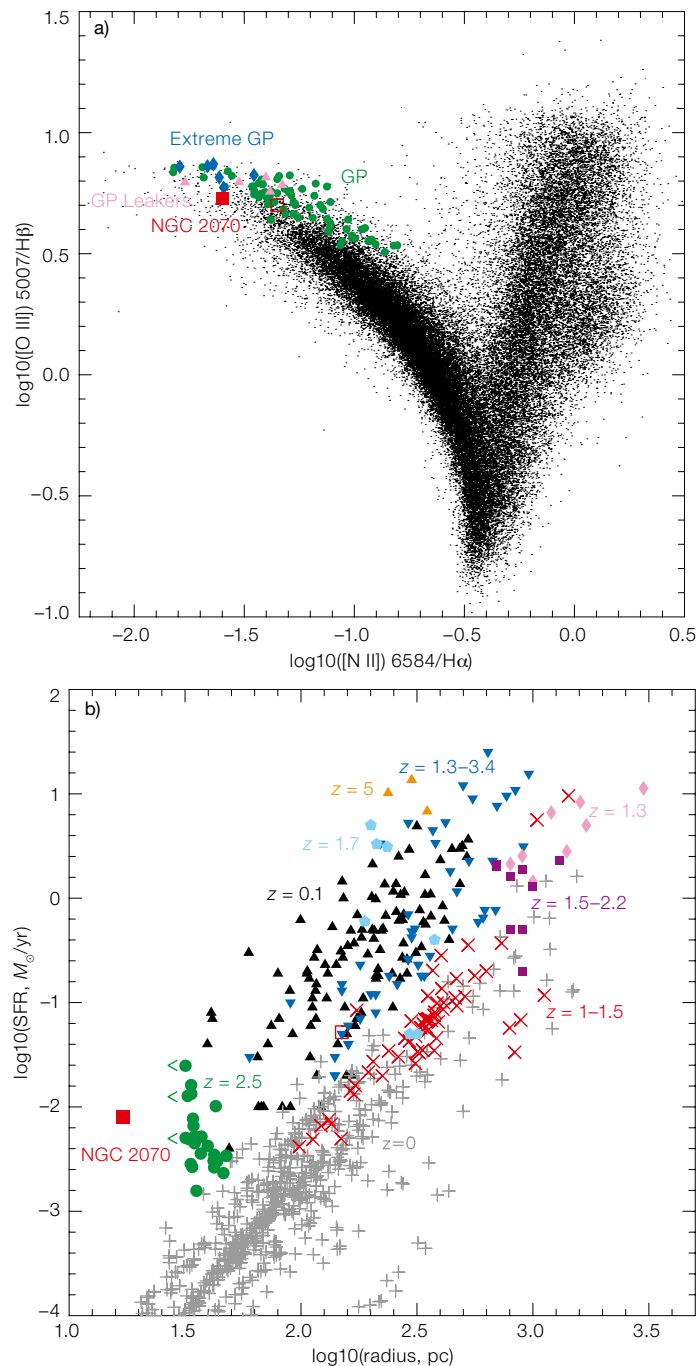


Figure 6. (a) BPT diagram (Baldwin, Phillips & Terlevich, 1981) illustrating the similarity in integrated strengths between NGC 2070/Tarantula (filled/open red square), Green Pea (green circles), extreme Green Pea (blue diamonds), and Lyman-continuum emitting Green Pea (pink triangles) galaxies, plus SDSS star-forming galaxies (black dots); updated from Figure 2 of Micheva et al. (2017). (b) Comparison between the integrated star-formation rate of NGC 2070/Tarantula (filled/open red square) and star-forming knots from galaxies, spanning a range of redshifts (adapted from Figure 2 of Johnson et al., 2017).